Supplemental Material for

Unveiling Process–Structure Mapping with a Deep Variational Autoencoder

Avanish Mishra Brenden William Hamilton Mashroor Shafat Nitol Nithin Mathew
Kipton Marcos Barros Timothy Clark Germann Saryu Jindal Fensin

Los Alamos National Laboratory, Los Alamos, NM 87545, USA

{avanish, brenden, mash, mathewni, kbarros, tcg, saryu}@lanl.gov

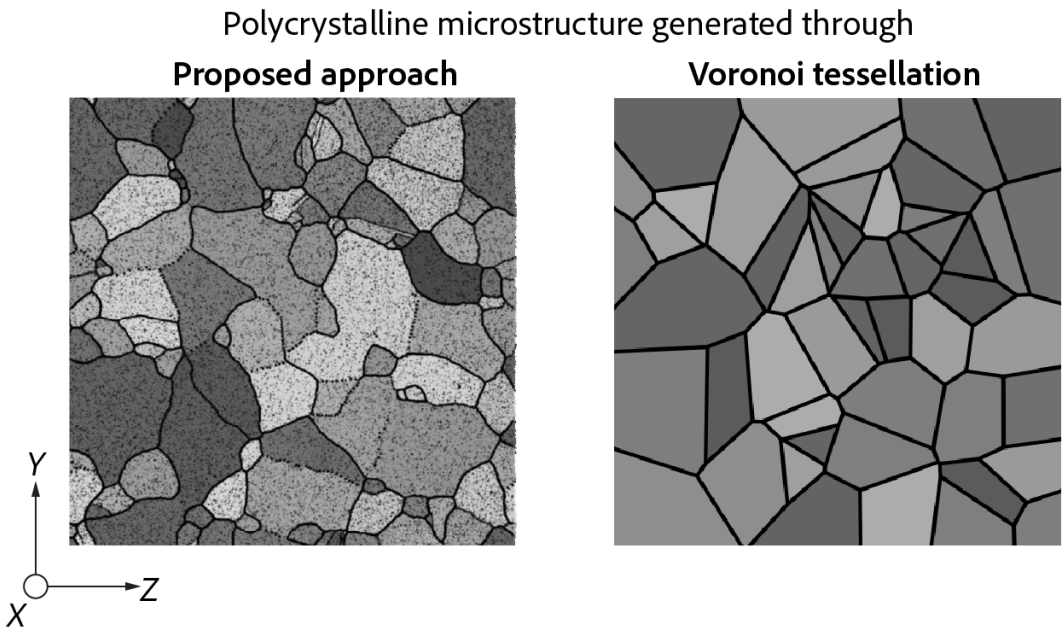

Figure S1. A 1 nm two-dimensional slice along the $Y-Z$ plane comparing the grain distributions produced by our method—with heterogeneous grain-size distributions, atomic segregation, and smooth interfaces—to those obtained using a Voronoi tessellation approach.

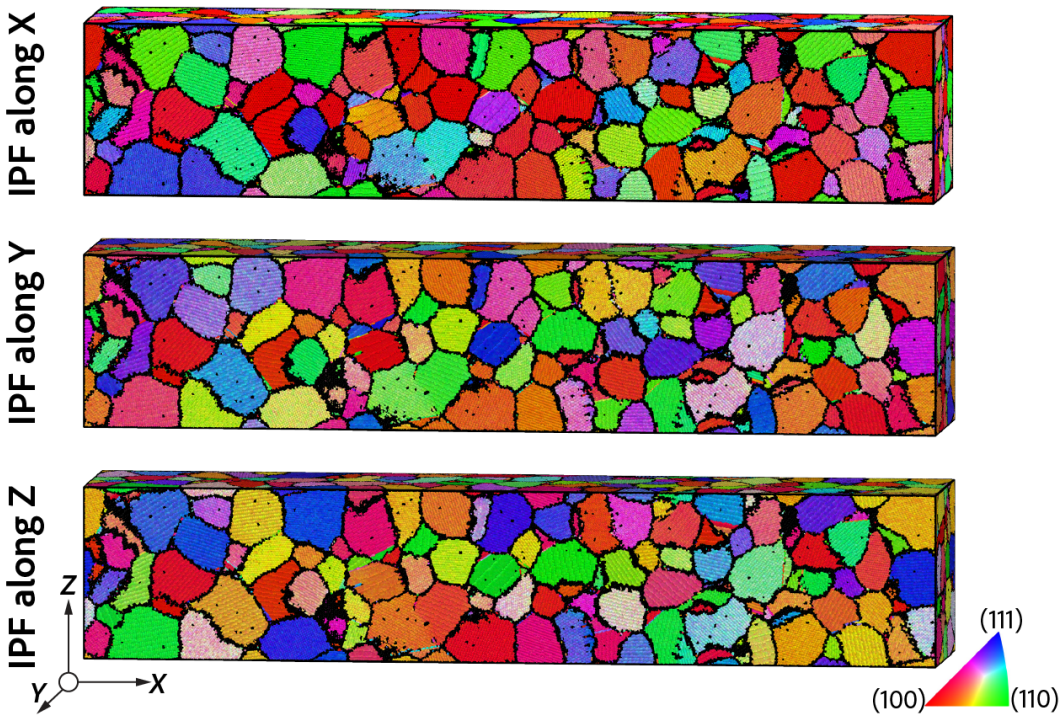

Figure S2. IPF colormap for a sample polycrystalline 3D microstructure generated along X ([1,0,0]), Y ([0,1,0]), and Z ([0,0,1]) axes. The change in grain color highlights crystal orientation along different directions.

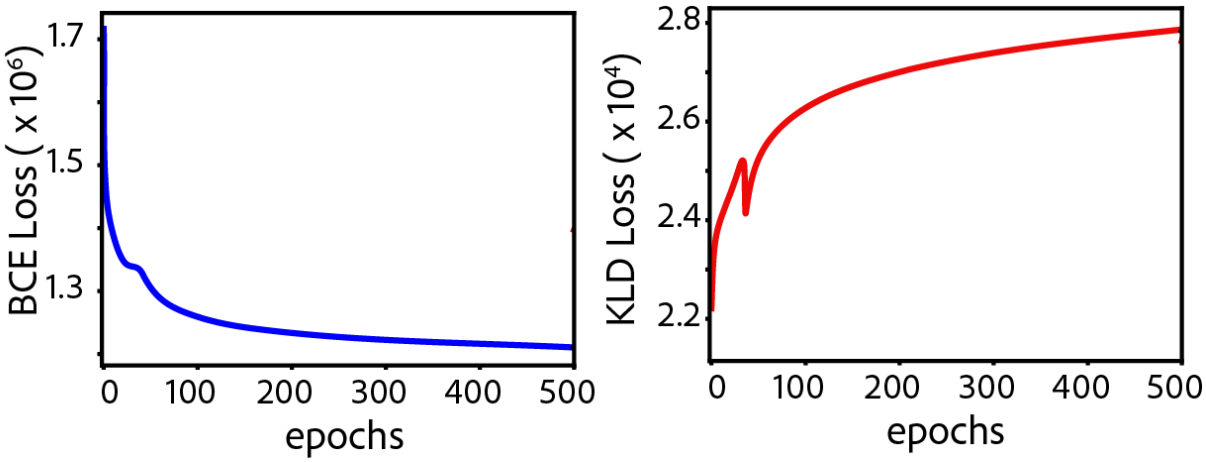

Figure S3. The reconstruction (BCE) and Kullback–Leibler divergence (KLD) losses during training as a function of epochs for models with 1 B parameters.

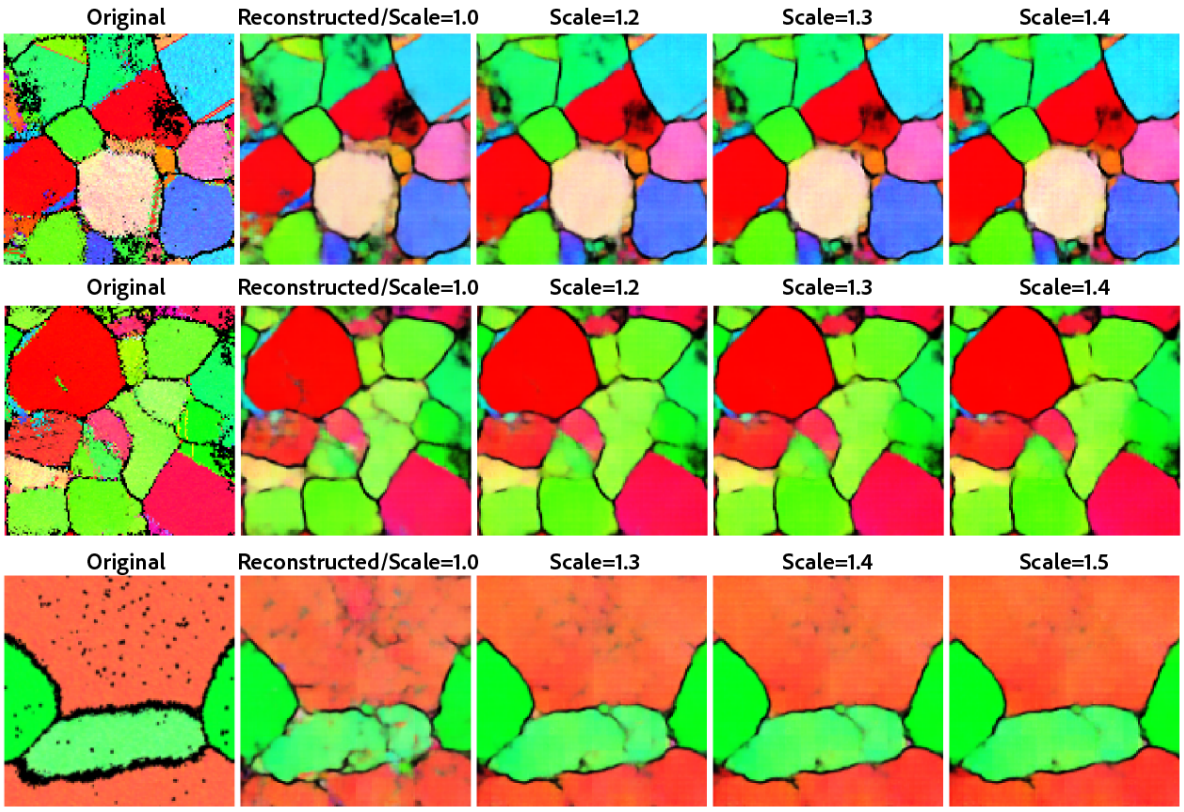

Figure S4. Reconstructed micrographs obtained by uniformly scaling the latent vectors prior to decoding, illustrating smoother grain boundaries and reduced noise.

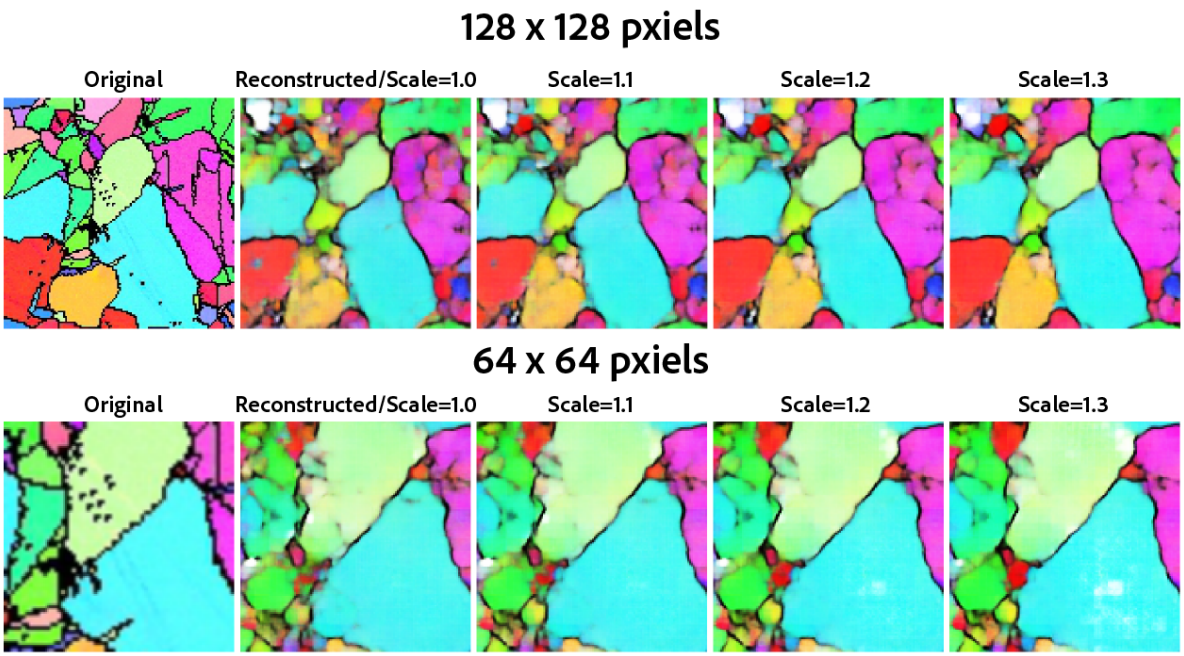

Figure S5. Reconstructed experimental Cu micrographs obtained by uniformly scaling the latent vectors prior to decoding, following cropping to two different sizes (128×128 and 64×64 pixels), corresponding to the images shown in Fig. 7(b).